Biol. Cybern. 66, 429–435 (1992)

Biological Cybernetics

Response transfer functions of *Limulus* ventral photoreceptors: interpretation in terms of transduction mechanisms*

Norberto M. Grzywacz [1,2], Peter Hillman [1], and Bruce W. Knight [3]

[1] Institute of Life Sciences, The Hebrew University of Jerusalem, Jerusalem 91904, Israel
[2] Smith-Kettlewell Eye Research Institute, 2232 Webster Street, San Francisco, CA 94115, USA
[3] The Rockefeller University, New York, NY 10021, USA

Received September 7, 1991/Accepted September 18 1991

Abstract. In recent years, our knowledge of the biochemical mechanisms underlying the transduction process in photoreceptors has expanded rapidly. However, a full picture of the temporal dynamics of these mechanisms remains elusive. To study the dynamics in the *Limulus* ventral photoreceptor, we measure its light-evoked transfer function under voltage clamp. Comparison of this transfer function to biochemically realistic theoretical models of transduction provides insights into the photoreceptor dynamics. This comparison supports the suggestion that the low-frequency behaviour of the *Limulus* photoreceptor, corresponding to light and dark adaptation, is that of a nonlinear negative feedback loop. The main reactions of this loop have time constants between about 1 and 40 s. Such a feedback loop does not account, however, for the high-frequency behaviour of the responses, which implies the existence of a further, fast-acting, mechanism.

Introduction

There have been great advances in the understanding of the transduction process in photoreceptors (reviewed by Bacigalupo et al. 1990). However, considerable gaps remain, especially in invertebrates. Here, involvement of Ca^{++} (Lisman and Brown 1972, 1975) and probably $InsP_3$ (Inositol Trisphosphate) (Fein et al. 1984; Brown et al. 1984) has been demonstrated, but their exact roles are still unclear and little attention has been paid to the chemical dynamics.

Linear analysis is a powerful tool in the study of photoreceptor dynamics (Pinter 1966; Dodge et al. 1968; Knight et al. 1970; Pasino and Marchiafava 1976; Toyoda and Coles 1975; Brodie et al. 1978). The recent growth of knowledge of the invertebrate transduction process provides a framework for a renewed application of the technique to the ventral photoreceptors of *Limulus*.

The approach is based on a measurement of the transfer function of these cells. Although photoreceptors are intrinsically nonlinear, they have been found to respond quite linearly to small modulations of light intensity around a fixed background (Knight et al. 1970). This linearization makes possible the application of standard linear-systems analysis to the system. The simplest method of carrying this out is the use of fixed-frequency sinusoidally modulated stimuli to determine the transfer function, that is, the relative amplitude and phase of the system's response as a function of modulation frequency. We present the results of such an experiment. New constraints on dynamic models of the transduction process result from this application.

We also review the theoretical basis of the technique, display the predictions of the theory for a number of elementary mechanisms, and offer a convenient format for the confrontation of theory and experiment.

Methods

The preparation, stimulation source, and recording methods were as described in Grzywacz and Hillman (1988). Complete experiments were performed on six cells. All measurements were done at room temperature (21–23°C).

The stimuli in this study were sinusoidally modulated about a mean. The light source was a green light-emitting diode (LED, solid-state lamp 4958 Hewlett–Packard). In LEDs, the relation between current and luminous emission is highly linear. However, the dependence of forward-biased current on voltage in solid-state diodes is nonlinear. Only for voltages exceeding the junction potential does the relation approximate linearity, so we operated the LED only at such voltages. These voltages corresponded to currents higher than 10 mA. The specified allowable maximum is 30 mA, so we stayed in the range 10–30 mA. The

* This work was supported by grants from the Binational Science Foundation (BSF) Jerusalem, Israel and the Israel Academy of Sciences and Humanities, by NIH grant EY 1428, and by NSF grant DMS 8505442

electronic circuit and the linearity measurements we used were similar to those suggested by Nygaard and Frumkes (1982). The D.C. and sinusoidal A.C. voltage were supplied by the computer to an operational amplifier in a follower configuration. The output of the follower drove an *npn* transistor in a common emitter configuration, and the transistor supplied the currents to the LED (Senturia and Wedlock 1975). The linearity of the LED system was determined by comparing its luminous emission as measured by a linear photoelectric cell to the voltage supplied to the system. The output of the photoelectric cell and the supplied voltage coincided well up to a modulation depth of 40%, indicating linearity of the system up to this modulation. (The depth of modulation is defined as half the ratio of the peak-to-peak amplitude, $2I_1$, to the mean, I_0.)

The computer sampled the signals at 30.5 μs intervals, and the averages of 128 consecutive samples were stored. This procedure corresponded to a sampling rate of 256 Hz and was chosen to provide high-frequency filtering and to minimize the problems of aliasing. (The high rate of sampling was needed for noise analysis of the responses as reported in Grzywacz et al. 1988; see companion paper, Grzywacz et al. 1992.)

After successful cell penetration, the photoreceptor was allowed to dark adapt for 30 min. Then, low intensity 30 s steps of light were presented to the cell and the intensity found at which about 1 bump/s was observed (a bump is thought to be the response to a single photon. We call this intensity I_b. The experiment then consisted of repeated series of six runs. Each run was composed of thirteen divisions as defined below. The baseline was determined for each division separately, by averaging 2 s patches of signal, 1 s before and 1 s after the stimulus, to avoid the contribution of possible drifts. After the baseline was measured, a 30 s step of light was delivered to the cell to adapt it to its new mean level. During this 30 s no recording was made. Each new mean level was ten times the preceding one, up to $10^5 I_b$.

In each division, immediately after the end of the steady stimulus, a different frequency of sinusoidal modulation was initiated simultaneously with recording. In the first division, the frequency was 32 Hz and in the next eleven divisions the frequency was successively reduced by a factor of two, so that in the twelfth division, the frequency was 1/64 Hz. The frequency in the thirteenth division was 1/256 Hz. The number of cycles recorded was 64 for the six first divisions and was reduced successively by factors of two over the next six divisions so that in the 12th division only one cycle was recorded. In the thirteenth division, too, one cycle was used, but in addition only one second in four was recorded, to a total of 64 s of actual recording.

For the first run, the background light intensity was $10I_b$. It was then successively raised by 1 log unit from run to run. Between successive series of runs there was a 15 min wait for dark-adaptation. Figure 1 shows the responses recorded in a typical experiment.

After the experiment, the successive response cycles of each of the first twelve run divisions were averaged to yield a mean response cycle for each division. For the thirteenth division, a response cycle of 64 time points was constructed by separately averaging each of the 64 one-second patches over which data were collected. The zeroth, first and second Fourier coefficients of these mean responses were then calculated. The average of the response, R_0, its modulation amplitude, R_1, and its phase relative to the stimulus were derived by standard methods from these Fourier coefficients (Pinter 1966).

In this paper, we accepted only cells in which R_0 did not change by more than 10% for any frequency between two consecutive series of runs. Usually, no significant amplitude modulation was observed for the 32 Hz frequency.

The amplitude of the transfer function is then defined as $H = (R_1/R_0)/(I_1/I_0)$, where I_0 and I_1 are the average and modulation amplitude of the stimulus respectively. By this definition, the transfer function is independent of the depth of stimulus modulation (within the quasi-linear range) and is also independent of the units of both stimulus and response.

The linearity of the system was checked by measuring the second harmonic content of the mean responses. It never exceeded 5% of the fundamental harmonic up to a modulation depth of 40%. In this range, $|H|$ was observed to be independent of the modulation depth; our working modulation was 25%.

According to the definitions of $|H|$ given above, the logarithms of R_0 and I_0 yield a curve whose slope, at any point I_0, is the asymptotic value of $|H|$ at zero frequency and at intensity I_0. In the range of intensities covered, the steady-state stimulus-response curve proved to be a power law (Grzywacz and Hillman 1988): $R_0 = aI_0^n$ with $n < 1$. We plotted R_0 as a function of I_0 on a log–log scale to obtain the value of this asymptote. The phase asymptote of H is necessarily zero or π.

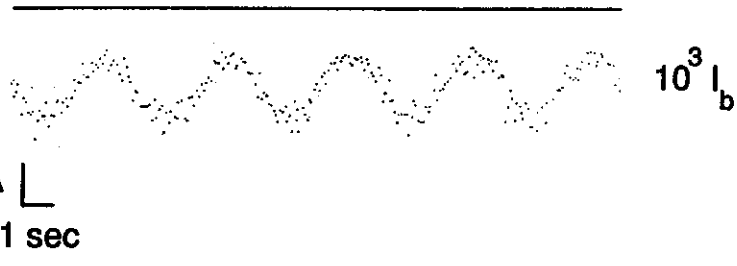

Fig. 1. Section of a typical intracellular voltage-clamped recording from a *Limulus* ventral photoreceptor. Each point represents the average of 128 consecutive samples which cumulatively span 3.904 ms. Every twentieth point is shown. The mean intensity corresponds to about 100 bumps/s, the modulation rate 0.25 Hz, and the modulation amplitude 25%. The solid line is the response's baseline, with inward currents plotted downwards. At the start of the trace, the intensity was equal to its mean value and was rising

For our purposes, a helpful graphical display of the system's response to small sinusoidal variations of input is the polar graph or "Nyquist Plot", in which the amplitude ratio between output and input is indicated at each frequency as a radial distance from the origin (zero response) and the corresponding angle is the phase difference between output and input at that frequency (Ahlfors 1979). If frequency points are labeled, this single display carries the same information as the more familiar pair of curves, amplitude and phase versus frequency, of the "Bode Plot", with the further advantage that particular response features take the form of visually vivid characteristic curves. On a Nyquist plot, for instance, we show below that the dynamics of a single-step chemical reaction corresponds to a semicircle whose zero and infinite frequency termini lie respectively on the horizontal axis and at the origin. Combinations of such reactions lead to other characteristic, and simple, curves. Comparison of the experimental data with these curves, and with the distribution of frequency points along them, constitutes a useful identification test and also assigns time constants to identified processes.

Results

Figure 2 displays the transfer function observations for six cells at one intensity (the lowest). The circle has unit radius. The data points for the six cells are connected to their central estimate at each stimulus frequency. (This estimate is the "complex median", the point which has the minimum sum of distances to the data points. For data points falling on a straight line, the central estimate reduces to the median, with which it shares the insensitivity to the positions of the least typical points.)

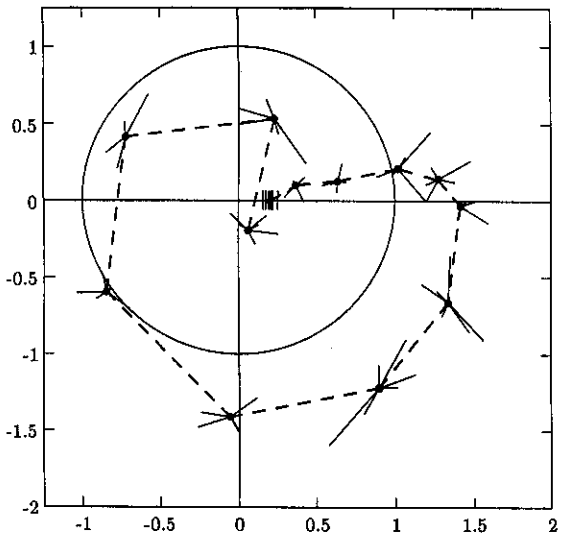

Fig. 2. Transfer function data from six cells at mean intensity eliciting about 10 bumps/s. The six points at each frequency are connected to their central estimate (see text). The display is the polar or Nyquist plot, in which amplitude ratio is displayed as distance from the origin and phase lag is plotted as angle of rotation clockwise starting at the positive horizontal axis. The unit circle is displayed. Six vertical lines surround the zero-frequency steady-state point, which is labeled by a 0 in the next figure. (These lines were derived for each intensity as described in the text.) Then, starting in the upper right quadrant with the set near this point, the frequencies used were 1/256, 1/64, 1/32, 1/16, 1/8, 1/4, 1/2, 1, 2, 4, 8, and 16 Hz labeled respectively, 1, 2, 3, 4, 5, 6, 7, 8, 9, 10, 11 and 12 in the next figure

While there is some scatter among the points, the general form of the transfer function is well-defined. Suppressing the extreme cells or extreme points in each set did not appreciably alter the functions. These comments apply equally at the other intensities. The zero frequency points on the x-axis are derived from the plot of the average response versus the average stimulus as described in the preceding section.

Figure 3a–e shows the transfer functions at five intensities with the frequency at each point indexed and given in the figure legend. The data points are the central estimates for six cells. Finally, Fig. 4 collects these curves on one graph for comparison.

Theory

In order to extract the maximal information from the data, we shall now develop the necessary theoretical framework. We shall then calculate the theoretical transfer function for a single first-order enzymatic reaction. Finally, we shall sketch the results of combining such reactions in series, parallel, and feedback configurations.

We first describe a system in which a single first-order chemical step leads from the presence of one chemical species to the creation of another. For instance, the first species might be an enzyme, which creates a decaying product from a large pool of substrate. If B is the departure of the concentration of this product from equilibrium, and A is proportional to the departure of the concentration of the causative chemical from equilibrium, then we may write

$$\tau \, dB/dt = -B + A \,, \tag{1}$$

where τ is the time constant for removal of B near that equilibrium. Suppose the time course of A is sinusoidal given by the real part of $A = A_0 \exp(i\omega t)$, where $\omega = 2\pi f$ with f the sinusoid's frequency.

Then B responds sympathetically as $B = B_0 \exp(i\omega t)$, from which follows $dB/dt = i\omega B$, and (1) gives

$$B/A = 1/(1 + i\omega\tau) \tag{2}$$

This complex number fixes both the amplitude ratio and the phase-shift between the departures from equilibrium of the two chemical species. Equation 2 may be regarded as a fractional-linear function of a complex variable ω, and therefore maps lines on the complex ω-plane to circles on a Nyquist graph of B/A. In particular, the set of positive real ω values maps to a semicircle, which lies below the real axis of the B/A plane and has the real termini $B/A = 1$ at $\omega = 0$ and $B/A = 0$ at $\omega \to \infty$. We also observe from (2) that the imaginary

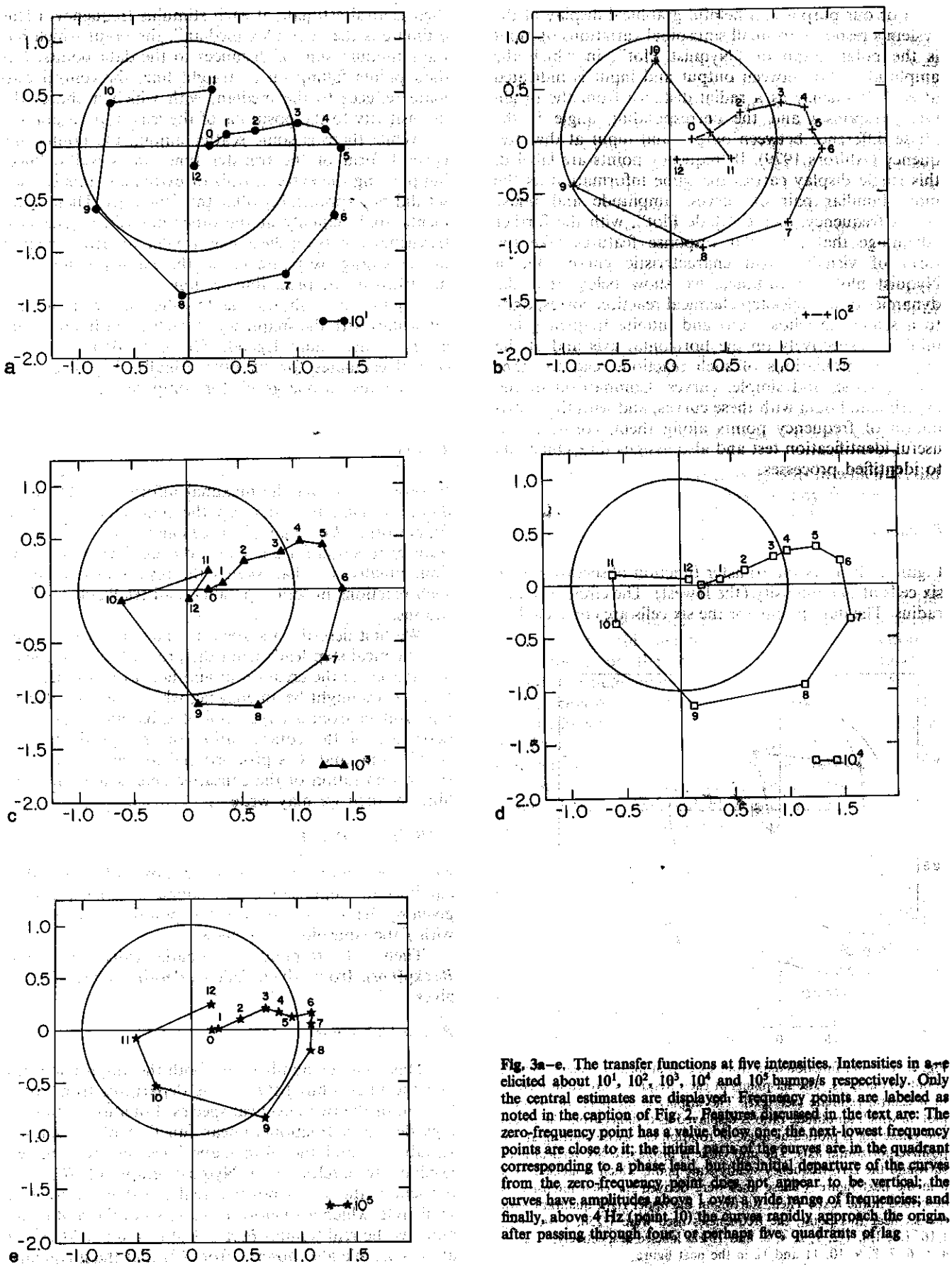

Fig. 3a–e. The transfer functions at five intensities. Intensities in a–e elicited about 10^1, 10^2, 10^3, 10^4 and 10^5 bumps/s respectively. Only the central estimates are displayed. Frequency points are labeled as noted in the caption of Fig. 2. Features discussed in the text are: The zero-frequency point has a value below one; the next-lowest frequency points are close to it; the initial parts of the curves are in the quadrant corresponding to a phase lead, but the initial departure of the curves from the zero-frequency point does not appear to be vertical; the curves have amplitudes above 1 over a wide range of frequencies; and finally, above 4 Hz (point 10) the curves rapidly approach the origin, after passing through four, or perhaps five, quadrants of lag

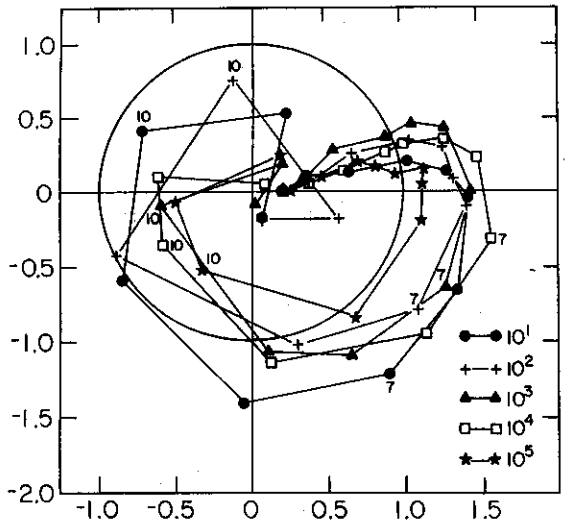

Fig. 4. The curves of Fig. 3 replotted together, (with frequency labeled only at two frequencies) to facilitate comparison. At the highest intensity, the modulation is considerably reduced and the response speeded up

part of B/A becomes the negative of its real part when $\omega = 1/\tau$. Thus, the driving frequency f_1 that yields a 45° phase-lag, and that reduces the amplitude ratio from its zero-frequency value by a factor of $1/\sqrt{2}$, measures the dynamical time constant in (1) as $\tau = 1/2\pi f_1$.

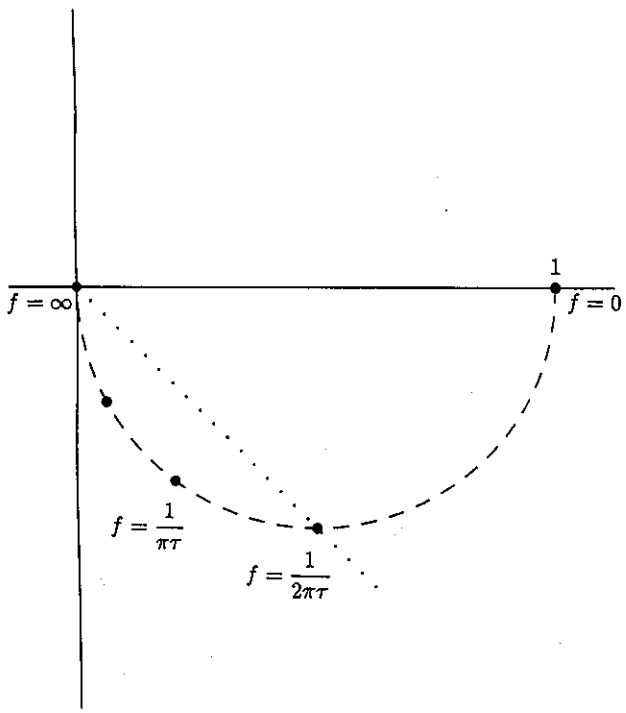

Fig. 5. A Nyquist graph of the theoretical transfer function for a single-step chemical reaction. The function is a semi-circle with frequency points falling as indicated, where τ is the time constant of the chemical reaction. The dotted line indicates the f_1 frequency, which is discussed in the text after (2). The graph shows that the Nyquist display of the transfer function of a simple reaction has a simple and easily recognizable form

Figure 5 displays this result and also labels the frequency points. The same sample curve is obtained for any single-step process irrespective of the order of its kinetics, since any such process can be linearized for small modulations.

This result provides evidence of mechanism. A transfer function that conforms to such a curve in both shape and frequency points may be assumed to arise from a process which is dominated by one single-step reaction with a particular time constant.

We now display, without derivation, further examples of such curves, in which other stages are added, and comment on their features. If two stages in series have very different time constants, the transfer function shape will be determined largely by the slower stage. If the time constants are comparable, but different, a new and less simple curve results. If they are the same, the curve is changed but remains simple. For instance, if two reactions in series have similar time constants, the graph of Fig. 6b results. (Figure 6a reproduces the curve of Fig. 5 for comparison). Each additional series stage adds a $\pi/2$ phase lag to the final approach to the origin. However, the transfer function's amplitude decreases rapidly with frequency, even for equal time constants, so that large phase lags may not be observed in practice. Nevertheless, the number of quadrants through which the function is observed to pass sets a

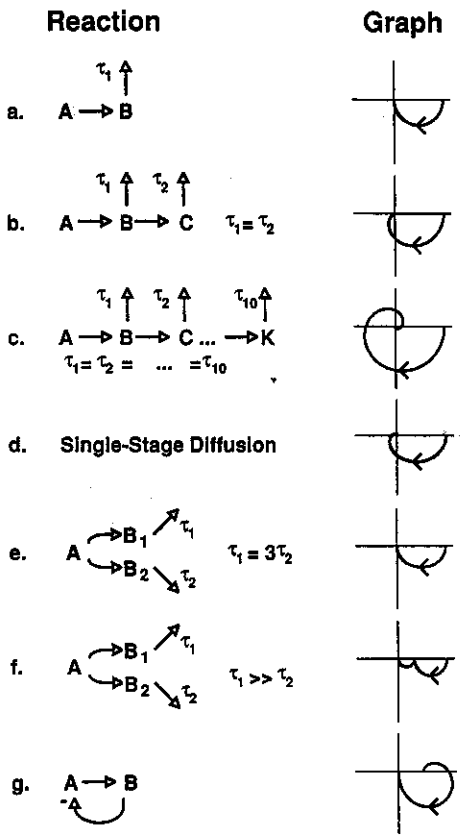

Fig. 6. Nyquist graphs of the theoretical transfer functions as calculated for various chemical-reaction chains, as indicated. The arrows indicate enzymatic amplifications or product decay, the τ are the decay time constants, and the feedback in *g* is a linear subtraction

lower limit on the number of stages in the process. The curve for ten series stages with comparable time constants is shown in Fig. 6c.

A case of particular interest is that of a single stage of diffusion of a decaying material. In three dimensions, diffusion resembles an infinite number of parallel chains each with an infinite number of fast stages in series. These stages are not identical, however, to those of Fig. 6a, b and c, since both forward and backward reactions occur. Nevertheless, the graph for diffusion spirals inwards indefinitely, as would be expected from an extension of Fig. 6c to infinite stages. Figure 6d displays a Nyquist plot for one-dimensional diffusion.

The next case is one in which the input chemical species leads in parallel to the creation of the two output sub-species, counted as one for the transfer function, but with possibly different decay time constants. If the constants are similar, the curve is as before – Figs. 5 and 6a. If they are different, the curve depends on the division between the two parallel paths: If this division is such that the populations of the two sub-species are created at relatively similar rates, the curves of Fig. 6e and f arise for the case in which one time constant is a little larger or much larger than the second, respectively. In Fig. 6f, the ratio of the diameters of the two semicircles is proportional to the ratio of the equilibrium populations of the two sub-species.

A final illustration is that of Fig. 6g, in which a single linear negative (subtractive) feedback reaction is joined to a single forward reaction. The feature that distinguishes this curve from all the others is the initial phase lead. While other mechanisms can cause initial phase leads, this lagged negative feedback is a simple and common case, so such a mechanism should be suspected whenever an initial phase lead is observed.

All these curves (Fig. 6a–g) start at a point on the positive x-axis (zero phase lag) – at sufficiently low frequencies any reasonable physical process will be able to follow the stimulus modulation exactly in phase (or with a phase shift of π if input increment leads to output decrement). The amplitude of this point is the slope of the steady-state stimulus-response curve.

Another common feature of all these curves is that they ultimately (for sufficiently high frequencies) spiral clockwise into the origin. This too, is a characteristic of any well-behaved physical process.

All the plots show an initial pure phase change, that is, an initial vertical slope, either downwards or, if there is a negative feedback loop, upwards. (The fractional power-law case of Thorson and Biederman–Thorson (1974) has a singular point at zero frequency and does not conform to this generalization. More trivially, high- and band-pass filters also do not, as they start at zero.) On the other hand, the final approach to the origin is generally a pure amplitude change, with a fixed phase which depends on the number of stages in series: A phase lag of $\pi/2$ is added for each of these stages.

In summary these displays indicate individual signatures which provide tools for characterizing the mechanisms that underlie a transducing system.

Discussion

We now comment on the interpretation of the features in the experimental data, comparing them with the theoretical predictions for various mechanisms.

The "zero frequency" experimental point, which was obtained from the log vs. log slope of the steady-state response curve as discussed above, is about 0.2 at all intensities, reflecting the light adaptation of the cell and the sublinear (fractional power law) steady-state stimulus-response curve (Grzywacz and Hillman 1988).

The lowest-frequency points (1/256 Hz) depart only slightly from this "zero-frequency" point. This suggests that there are no relevant elements in the biochemical cascade with time constants longer than a few minutes. This observation agrees with that of Grzywacz and Hillman (1988) that with steady stimuli "the responses were found to stabilize after around 5 min of illumination".

The steady increase in amplitude of the transfer function between about 1/256 Hz and 1/8 Hz or 1/4 Hz indicates that the main reactions of the feedback loop have time constants in this range (about 1 to 40 s).

The observation that the points in this region all exhibit a phase lead suggests that the adaptation process may involve a negative feedback (see Fig. 6g). The wide range of frequencies over which a phase lead is observed (especially at high intensities) is consistent with a simple high-gain feedback loop if the feedback has a large spread of delays and these delays are long compared with the forward time.

One feature of the experimental data is not seen in the theoretical curves: At low frequency the experimental transfer function appears to depart from its zero frequency point on the real axis at an angle that is not a right angle. Such a feature is characteristic of a frequency response that contains the summed responses of several parallel components that have among them a distribution of time-constants, some of which fall below the period of the slowest measuring frequency and consequently contribute outputs with substantial phase-shift. An example of this situation has been discussed by Thorson and Biederman-Thorson (1974); a further important example may be diffusion.

We next refer to the high-frequency behaviour of the curve. The rapid decline of the amplitude above about 4 Hz indicates that at least one rate-limiting step in the cascade has a time constant of about $1/(2\pi 4\text{ Hz})$ or 40 ms. The phase lag at which the amplitude becomes small is about 2π, or four quadrants. For a system of sequential stages, four is then the minimum number of stages (see discussion of Fig. 6b and c).

The amplitudes of the transfer functions are above 1 for part of their intermediate range. This is consistent with a negative feedback which shows an effective delay in its impulse response. Near the frequency at which

this delay is a half-cycle, such a feedback enhances maxima and depresses minima, resulting in a transfer function amplitude above 1.

However, the range of frequencies over which such an enhancement would persist spans only about a factor of three. The data, on the other hand, exhibit an amplitude enhancement above 1 over a wide range, from below 1/16 Hz to above 1 Hz. A possible source of this broad range is a biphasic adaptation effect: An "adaptive" influence which initially enhances the response and only later depresses it. We speculate that such an enhancement may be due to the same mechanism that mediates the supralinearity of flash responses (Grzywacz et al. 1988).

A quantitative analysis of the dynamics of the responses of the *Limulus* lateral eye eccentric cell has been represented by Thorson and Biederman-Thorson (1974). They were able to account for both the Weber–Fechner type steady-state stimulus-response relation, which this cell shows, and the cell's transfer function, which follows a power law in frequency at low frequency. To do so, they postulated a weighted sum of exponential relaxation processes, each with an exponential time course but with rate constants spread over a broad range. They predicted the range of the rate constants and the weighting of individual processes from the substantial progressive attenuation of illumination as it passes through the eccentric cell. The ventral photoreceptor is much more transparent, and it is encouraging to the Thorson's general suggestions that the amplitude of its transfer function, in contrast to that of the eccentric cell, approaches a finite fixed value at low frequency.

The present approach has been extended by us (see companion paper, Grzywacz et al. 1992) to the study of separate portions of the transduction chain by application of a new dynamic noise analysis technique (Grzywacz et al. 1988). This technique extracts from the observations the properties of the single photon responses that underlie the overall response. Transfer function analysis applied to these properties yields a characterization of various components of the transduction chain, and therefore makes possible more detailed conclusions about the feedback process than those that can be reached from observations of the overall response only.

Acknowledgements. We thank Consuelita Correa-Grzywacz for help with the figures.

References

Ahlfors L (1979) Complex analysis. McGraw-Hill, New York

Bacigalupo J, Johnson E, Robinson P, Lisman JE (1990) Second messengers in invertebrate phototransduction. In: Hidalgo C, Bacigalupo J, Jaimovich E, Vergara J (eds) Transduction in biological systems. Plenum Press, New York

Brown JE, Rubin LJ, Ghalayani AJ, Tarver AL, Irvine RF, Berridge MJ, Anderson RE (1984) Myo-inositol polyphosphate may be a messenger for visual excitation in *Limulus* photoreceptors. Nature 311:160–162

Brodie SE, Knight BW, Ratliff F (1978) The response of the *Limulus* retina to moving stimuli: a prediction by Fourier synthesis. J Gen Physiol 72:129–166

Dodge FA, Knight BW, Toyoda JI (1968) Voltage noise in *Limulus* visual cells. Science 160:88–90

Fein A, Payne R, Corson DW, Berridge MJ, Irvine RF (1984) Photoreceptor excitation and adaptation by inositol 1,4,5-trisphosphate. Nature 311:157–160

Grzywacz NM, Hillman P (1988) Biophysical evidence that light adaptation in *Limulus* photoreceptors is due to a negative feedback. Biophys J 53:337–348

Grzywacz NM, Hillman P, Knight BW (1988) The quantal source of area supralinearity of flash responses in *Limulus* photoreceptors. J Gen Physiol 91:659–684

Grzywacz NM, Hillman P, Knight BW (1992) The amplitudes of unit events in *Limulus* photoreceptors are modulated from an input that resembles the overall response. Biol Cybern (this issue)

Knight BW, Toyoda JI, Dodge FA (1970) A quantitative description of the dynamics of excitation and inhibition in the eye of *Limulus*. J Gen Physiol 56:421–437

Lisman JE, Brown JE (1972) The effects of intracellular iontophoretic injection of calcium and sodium ions on the light response of *Limulus* ventral photoreceptors. J Gen Physiol 59:701–719

Lisman JE, Brown JE (1975) Effects of intracellular injection of calcium buffers on light adaptation in *Limulus* ventral photoreceptors. J Gen Physiol 66:489–506

Nygaard RW, Frumkes TE (1982) LEDs: convenient, inexpensive sources for visual experimentation. Vision Res 22:435–440.

Pasino E. Marchiafava PL (1976) Transfer properties of rod and cone cells in the retina of the tiger salamander. Vision Res 16:381–386

Pinter RB (1966) Sinusoidal and delta function responses of visual cells of the *Limulus* eye. J Gen Physiol 49:656–693

Senturia DS, Wedlock BD (1975) Electronic circuits and applications. Wiley, New York

Thorson J, Biederman-Thorson M (1974) Distributed relaxation processes in sensory adaptation. Science 183:161–172

Toyoda JI, Coles J (1975) Rod response to sinusoidally flickering light. Vision Res 15:981–983

Dr. Norberto Grzywacz
Smith–Kettlewell Institute
2232 Webster Street
San Francisco, CA 94115
USA